Two-Particle Distribution and Correlation Function for a 1D Dusty Plasma Experiment

Amit K. Mukhopadhyay and J. Goree

Phys. Rev. Lett. **109**, 165003 — Published 18 October 2012

DOI: 10.1103/PhysRevLett.109.165003

Two-particle distribution and correlation function for a 1D dusty plasma experiment

Amit K. Mukhopadhyay and J. Goree
Department of Physics and Astronomy, The University of Iowa, Iowa City, Iowa 52242
(Dated: September 7, 2012)

Experimentally measured velocities are used to obtain the one- and two-particle distribution functions, f_1 and f_2 and the two-particle correlation function $g_2 \equiv f_2 - f_1 f_1$. The fluctuating velocities of interacting charged microparticles were recorded by tracking their motion while they were immersed in a dusty plasma. The phase space was reduced by having only two particles in a harmonic one dimensional (1D) confining potential. In statistical theory, g_2 is usually said to be dominated by the randomness of collisions, but here we find that it is dominated by collective oscillatory modes.

PACS numbers: 52.27.Lw, 52.25.Dg, 05.20.Dd, 05.40.Jc

Interacting particles that are confined to one dimensional (1D) motion, so that one particle cannot pass another, are found in many systems. These include optically-confined colloidal particles in an aqueous solution [1, 2], a chain of ions in a storage ring [3], Wigner crystals consisting of electrons confined to quantum wires [4], atoms on carbon nanotubes [5], microfluidic crystals [6], ball bearings in channels [7], dusty plasmas [8, 9], and single-channel ion flow across biological membranes [10]. To be one dimensional, these systems require a confinement force so that one particle does not cross another [11]. Some of these systems also have a thermal bath.

The combination of a confining force and a thermal bath can lead to a battle between probabilistic and deterministic motion. In our experiment, there are two microparticles. Their motion is partly probabilistic, i.e., stochastic, because they are immersed in a gas of many atoms; and they are partly deterministic because they are confined in an electrical potential well. The two microparticles are charged and interact with one another through an electrical repulsion. As was pointed out by van Zon and Cohen [12], in a colloid the greater mass of a microparticle as compared to the molecules in the surrounding liquid allows the many-particle problem to be simplified; the effect of the molecules can be considered as contributing only to friction and Brownian motion of the microparticle, even when the microparticle also experiences confining forces. The same simplifying principle applies to our experiment, with its microparticles immersed in a partially ionized gas. In our experiment, we will describe the battle of probabilistic and deterministic motion using experimentally determined particle distribution functions.

A many-particle system is described by an N-particle distribution function f_N in the statistical theory of gases [13], liquids [14] and plasmas [15]. As it is used in the Liouville equation [15], f_N represents the probability per unit volume of finding the system, at a given time, somewhere in the $6N$ dimension phase space defined by the positions and velocities of all N particles. A smaller phase space can be used by averaging f_N, as in the BBGKY hierarchy [15, 16], yielding distribution functions, f_1 and f_2 for one and two particles, respectively. Here $f_1(\alpha)$ is the probability per unit volume in 6D phase space of finding any particle α at a specified position and velocity, while the two-particle distribution $f_2(\alpha, \beta)$ is a joint probability for particles α and β to be found at $\mathbf{x}_\alpha, \mathbf{v}_\alpha$ and $\mathbf{x}_\beta, \mathbf{v}_\beta$. To describe the interactions of particles, for example due to collisions, one invokes

$$\begin{aligned} f_2(\mathbf{x}_\alpha, \mathbf{v}_\alpha, \mathbf{x}_\beta, \mathbf{v}_\beta, t) &= f_1(\mathbf{x}_\alpha, \mathbf{v}_\alpha, t) f_1(\mathbf{x}_\beta, \mathbf{v}_\beta, t) \\ &+ g_2(\mathbf{x}_\alpha, \mathbf{v}_\alpha, \mathbf{x}_\beta, \mathbf{v}_\beta, t), \end{aligned} \tag{1}$$

which is called a cluster expansion [14] or cumulant expansion [17]. Here, g_2 is a correlation function that is non-zero if the particles interact or zero if they move independently. Positive and negative values of g_2 indicate events that are more or less probable, respectively, than is typical. For many-body systems including non-ideal gases [13, 18], liquids [14], and weakly-coupled plasmas [15], Eq. (1) is accompanied by cluster expansions for higher-order distribution functions f_N. (We note that since strongly-coupled plasmas can behave like non-ideal gases or liquids, it would be reasonable to use them in that case as well.) For these many-body systems it is generally necessary to make the approximation of truncating the cluster expansion at some level [15], but in this paper the experiment has only two microparticles, which allows us to use Eq. (1) exactly without any truncation.

While f_2 and g_2 have prominent places in the *theory* for statistical physics of gases and plasmas that are dense enough that collisions are significant, they have seldom been determined using velocities and measured in *experiments*. In our search of the literature, we have not found any previous determination of f_2 and g_2 in plasmas, or any other physical system, using experimental velocity data as we shall do in this Letter.

To measure f_2 and g_2, we designed an experiment that allows direct observation of the particles in a reduced phase space. We used two charged polymer microparticles, which were restricted to move mainly in only one dimension, and were tracked using video microscopy. Measuring the microparticle velocity and obtaining f_2 and

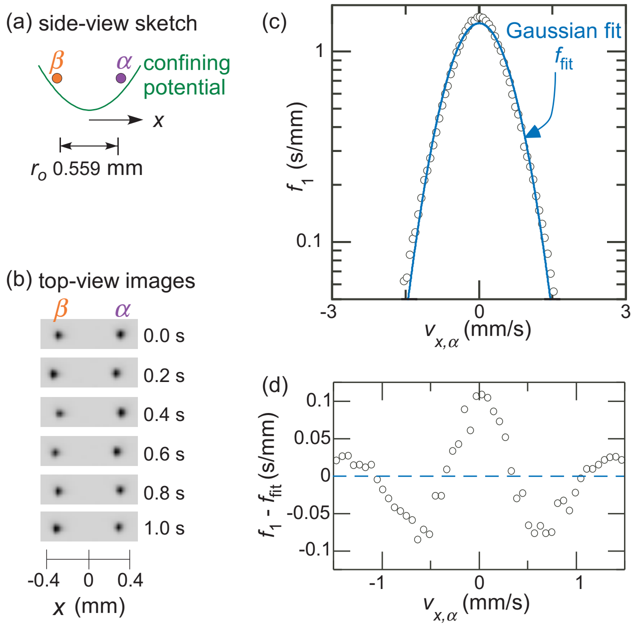

FIG. 1: (color online). (a) A side-view sketch of two microparticles, labeled α and β, in a harmonic confining potential. The microparticles move mainly along the x axis, and they oscillate in the confining potential. (b) Sequence of top-view images of the two microparticles [19] recorded by video microscopy, showing their small displacements with time. (c) The one-particle velocity distribution $f_1(\alpha)$ for microparticle α is presented as a histogram of velocity observations. It is slightly non-Gaussian; the deviation from a Gaussian fit is shown in (d) with an expanded scale.

g_2 in this experiment allows us to observe not only the probabilistic effects described by f_2 and g_2 in statistical theory, but also any coherent or deterministic motion arising from correlations in the motion of the particles. Probabilistic effects resembling Brownian motion are provided by the combination of collisions (with the large number of gas atoms that filled an entire experimental volume) and electrical fluctuations in the plasma. Deterministic effects in the motion also occur, because the two microparticles interact and are confined. In addition to the microparticles and gas, the experimental system included electrons and positive ions, which had a much smaller number density than the neutral gas atoms.

Our mixture of micron-size particles of solid matter, electrons, ions, and neutral gas atoms is called a dusty plasma [20]. The microparticles collect electrons and ions constantly, but in unequal number, so that they have a negative charge equivalent to several thousand electrons [21]. When the plasma is formed above a horizontal surface, such as an electrode, a boundary region of a few mm thickness is formed, which has a significant electric field that is capable of levitating the microparticles. This boundary region, called a sheath, conforms to the shape of the surface beneath it. By shaping the surface, one can confine clusters of a few particles [22–24]. The vertical displacements of the microparticles are so small, due to a strong vertical gradient of the sheath's electric field, that the motion is essentially limited to a horizontal plane.

In our experiment, the arrangement of microparticles is reduced to being 1D. This was done by shaping the sheath as shown in the Supplemental Material [19]. The two particles aligned along $\hat{x}$, with displacements that were largest along the x axis but much smaller in the other two directions, Fig. 1(a). A similar confinement was used in [25]. To generate a weakly ionized plasma, we applied 180 V peak-to-peak 13.56 MHz potentials between the lower electrode and the grounded vacuum chamber. Capacitive coupling was used so that a dc self-bias of -77 V developed on the lower electrode. The chamber was filled with argon gas at 13.5 mTorr pressure and 301 K temperature. Using a Langmuir probe located in the plasma near the particle location, the average electron energy was 2.4 eV with electron number density 2.8×10^{14} m^{-3}. The microparticles were 4.81 ± 0.08 μm diameter and $m = 8.93 \times 10^{-14}$ kg mass. The microparticles, which had a time-averaged spacing of $r_0 = 0.559 \pm 0.002$ mm, experienced Epstein drag as they moved through the neutral argon atoms, with a friction coefficient of 2 s^{-1} [26]. The microparticles were imaged from above at 100 frames/s, Fig. 1(a), and their positions and velocities were calculated as in [27]. Using a straight-forward adaptation of the method of Sheridan *et al.* [28] for 2D systems, we find $Q/e = -(4260 \pm 170)$ and $\kappa = 2.11 \pm 0.01$, where $\kappa \equiv r_0/\lambda_D$. Using the measured value r_0, we obtain $\lambda_D = 0.302 \pm 0.003$ mm [29]. Critical experimental parameters, including the dc self-bias and gas pressure, were verified to remain steady within measurement uncertainties during the observations.

Our system of two confined particles can be described by a phase space consisting of two positions and two velocities, which can be further reduced by averaging the distribution functions over position. This is suitable for our experiment since the microparticles mainly oscillate with small amplitudes about nearly fixed equilibrium positions (as can be seen in the video in the Supplemental Material [19]). Thus, we will analyze motion in the 2D subspace of $v_{x,\alpha}$ and $v_{x,\beta}$, which will allow us to more easily present results for f_2 and g_2 and use them to assess the competition between probabilistic and deterministic motion. In this reduced phase space, $f_1(v_{x,\alpha})dv_{x,\alpha}$ is the probability that particle α has a velocity in the range $v_{x,\alpha} < v_\alpha < v_{x,\alpha} + dv_{x,\alpha}$, and $f_2(v_{x,\alpha}, v_{x,\beta})dv_{x,\alpha}dv_{x,b}$ is the joint probability that particles α and β have velocities in the ranges $v_{x,\alpha} < v_\alpha < v_{x,\alpha} + dv_{x,\alpha}$ and $v_{x,\beta} < v_\beta < v_{x,\beta} + dv_{x,\beta}$, respectively. The experimental conditions are constant, so that the distributions f_1 and f_2 are independent of time. In this reduced phase space, Eq. (1) is

$$f_2(v_{x,\alpha}, v_{x,\beta}) = f_1(v_{x,\alpha})f_1(v_{x,\beta}) + g_2(v_{x,\alpha}, v_{x,\beta}). \quad (2)$$

We obtain the velocity distribution functions f_1, Fig. 1(b), as a histogram of observations of particle velocities. The data shown in Fig. 1(b) were obtained by binning all our measurements of the velocity of particle α. The steady conditions of the experiment allow us to use time averaging of data to serve as ensemble averaging. In Fig. 2(b), we present the product $f_1(\alpha)f_1(\beta)$, which appears in the cluster expansion Eq. (2). Unlike $f_1(\alpha)$ by itself, which is a function of only the velocity of particle α, the product $f_1(\alpha)f_1(\beta)$ is a function of the velocities of both microparticles. This product would represent the joint probability density if the two particles were independent in their motions. Next we will consider f_2, which includes the effects of the correlation g_2.

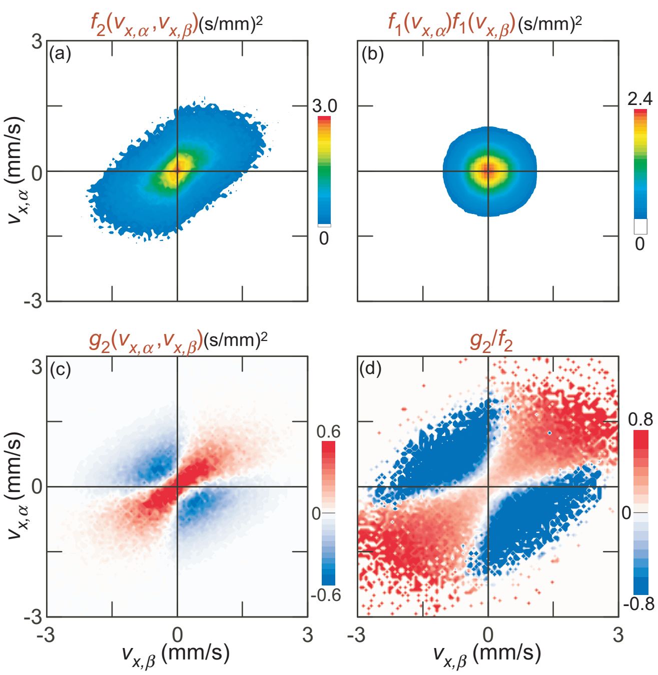

FIG. 2: (color online). (a) The two-particle velocity distribution function f_2, (b) the product of the one-particle distribution functions, and (c) the correlation function g_2, calculated using Eq. (2). Contours of $f_1(\alpha)f_1(\beta)$ are more circular than those of f_2. Positive correlations are shown in red (the color at the top of the color scale). (d) Alternate presentation of g_2 shown normalized by f_2. For example, if the value of g_2/f_2 is 0.6 at a specific location in phase space $v_{x,\alpha}v_{x,\beta}$, then correlated *dynamics* account for 60% of the two-particle distribution's value.

Our main results, the two-particle velocity distribution f_2 and correlation function g_2 in Figs. 2(a) and (c), reveal significant correlations. These correlations can be detected in f_2 by noting its non-circular contours, which are unlike the more circular contours of $f_1(v_{x,\alpha})f_1(v_{x,\beta})$ in Fig. 2(b). The correlations can be detected more conspicuously in g_2, which is calculated from f_2 using Eq. (2). We need a qualitative measure of the relative contribution of correlations. For this purpose, we find that the ratio g_2/f_2 is instructive, as shown in Fig. 2(d). This ratio reveals that the correlations are most significant at velocities > 1.0 mm/s. It is striking that as much as 50% or even more of f_2 is accounted for by the correlations at these higher velocities; for example at $v_{x,\alpha} = v_{x,\beta} = 1.5$ mm/s, g_2 represents $\approx 60\%$ of f_2.

Correlations are in general the result of interactions of nearby particles. In our experiment the microparticles interact constantly, like neighboring atoms in a solid. Since these interactions in a solid can sustain oscillations, or even waves like sound waves, we are motivated to examine our correlations for signatures of oscillations.

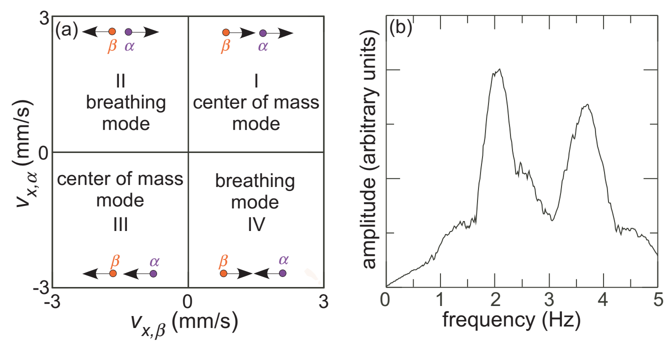

FIG. 3: (a) Labeling scheme for the quadrants of phase space according to the two types of oscillatory motion. (b) The frequency spectrum for the particle velocities, which is calculated as the square of the fast Fourier transform of the velocity time series for a particle. The frequency spectrum has two peaks, at 2.0 and 3.7 Hz, which we will identify as the center-of-mass and breathing modes, respectively.

With only two microparticles confined along a single axis, our system can sustain two kinds of oscillations. In the breathing mode, the two microparticles always move oppositely: toward one another (due to the confinement) and then away from one another (due to their mutual repulsion) [23, 24]. In the center-of-mass or sloshing mode [23, 24], the two microparticles move as one, oscillating back and forth in the confining potential. In the parameter space $v_{x,\alpha}v_{x,\beta}$ that we use in Fig. 2, if only a breathing mode is present, we would expect to observe events in only quadrants II and IV, where the two velocities are always opposite, as shown in Fig. 3(a). On the other hand, if only a center-of-mass mode is present, we would expect events to be observed in quadrants I and III, where the two velocities are in the same direction.

To examine our correlations for signatures of these two modes, we will take advantage of their different frequencies. In the frequency spectrum of the particle velocity, Fig. 3(b), we see two distinct peaks, at 2.028 ± 0.002 and 3.712 ± 0.005 Hz, which indicate the two modes of interest. Since most of the spectral power for velocity is concentrated in these two peaks, we expect that velocity correlations of two particles, as measured by g_2, will also be dominated by these two modes. To identify which peak corresponds to which mode, we apply a frequency bandpass filter to the velocities time-series data, as shown in the Supplemental Material [19]. We then recalculate f_1, f_2 and g_2. The results, for bandpasses that are centered on the two peaks, are shown in Fig. 4.

Figure 4 reveals features in the correlation g_2 that are distinctly different for the low and high-frequency bandpasses. For the low-frequency bandpass centered at 2.0 Hz, correlations are most positive in quadrants I and III, but for the high-frequency bandpass at 3.7 Hz they are most positive in quadrants II and IV. Recall that events associated with the center-of-mass mode are expected in quadrants I and III, leading us to identify the 2 Hz mode as the center-of mass mode. Likewise, we identify the 3.7 Hz mode as the breathing mode [30].

We find that the correlation g_2 is dominated not by randomness, but by motion associated with two modes. This result is contrary to the usual expectation in statistical theory for gases [13] and plasmas [15, 16]. If the motion had no deterministic character, we would expect g_2 in Fig. 2(c) to lack a distinct pattern. However, g_2 does have a distinct pattern. Moreover, after frequency filtering and then recomputing g_2 in Fig. 4, we find even more distinctive patterns in g_2 that are clearly attributable to the two modes: center-of-mass and breathing [31]. Thus, as a measure of the battle between deterministic and random motion, g_2 is dominated by the kind of modes that are most often thought of as deterministic [32].

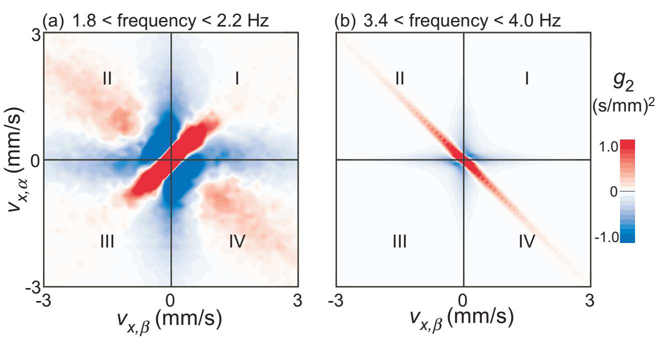

FIG. 4: (color online). Two-particle correlation function g_2 recalculated using frequency-filtered velocity time-series data. Different frequency bandpasses were chosen for (a) and (b) to correspond to the two peaks in the spectrum of Fig. 3(b). Features in g_2 are distinctly different for (a) and (b), which indicates that g_2 is dominated by the collective effects of two kinds of oscillations. To help distinguish the type of oscillations, the four quadrants I-IV are labeled as in Fig. 3(a). Comparing (a) and (b) to the labels in Fig. 3(a), we find that correlations arising from oscillatory motion at ≈ 2.0 Hz in (a) correspond to the center-of-mass motion, while correlations at ≈ 3.7 Hz in (b) correspond to the breathing mode.

In conclusion, we have used experimental data to obtain the two-particle distribution f_2 and calculate the correlation function g_2 using Eq. (2). For our dusty plasma, we find that g_2 has distinctive signatures of oscillatory modes. The experiment was designed so that two charged microparticles were immersed in a partially ionized gas with confinement to limit their motion to 1D, i.e., along a single axis without passing one another. Because of their charges, the two particles interacted constantly, and due to the confinement they had two oscillatory modes corresponding to center-of-mass and breathing motion. We find that the frequency spectrum for g_2 has distinctive signatures of the two oscillatory modes. Although the statistical theory of gases and plasmas often considers g_2 as an indicator of probabilistic effects associated with dissipation and collisions, in this experiment we find that g_2 is dominated by collective effects.

We thank E. G. D. Cohen, Y. Feng, M. Khodas, and B. Liu for helpful discussions. This work was supported by NASA and NSF.

[1] S. A. Tatarkova, A. E. Carruthers, and K. Dholakia, Phys. Rev. Lett. **89**, 283901 (2002).
[2] V. Karásek *et al.*, Phys. Rev. Lett. **101**, 143601 (2008).
[3] G. Birkl, S. Kassner, and H. Walther, Nature (London) **357**, 310 (1992).
[4] V. V. Deshpande and M. Bockrath, Nature Physics **4**, 314 (2008).
[5] M. T. Cvitas and A. Siber, Phys. Rev. B **67**, 193401 (2003).
[6] T. Beatus, T. Tlusty and R. Bar-Ziv, Nature Physics **2**, 743 (2006).
[7] G. Coupier, M. S. Jean, and C. Guthmann, Phys. Rev. E **73**, 031112 (2006).
[8] B. Liu, K. Avinash, and J. Goree, Phys. Lett. **91**, 255003 (2003).
[9] T. E. Sheridan, Phys. Scr. **80**, 065502 (2009).
[10] K. L. Kirk and D. C. Dawson, Journal of General Physiology **82**, 297 (1983).
[11] D. Lucena *et al.*, Phys. Rev. E **85**, 031147 (2012).
[12] R. van Zon and E. G. D. Cohen, Phys. Rev. E **67**, 046102 (2003).
[13] M. S. Green, J. Chem. Phys. **25**, 836 (1956).
[14] J. E. Mayer, *Statistical Mechanics*, 2nd ed. (John Wiley & Sons, New York, 1977), Chap. 9.
[15] D. R. Nicholson, *Introduction to Plasma Theory* (John Wiley & Sons, New York, 1983), Chap. 4.
[16] N. A. Krall and A. W. Trivelpiece, *Principles of Plasma Physics* (McGraw-Hill Book Company, New York, 1973), Chap. 7.
[17] L. E. Reichl, *A Modern Course in Statistical Physics*, 1st ed. (University of Texas Press, Austin, 1980), p. 357.
[18] Y. L. Klimontovich, Sov. Phys. Usp. **16**, 512 (1974).
[19] See Supplemental Material at XXXX for a photograph of the lower electrode setup (Fig. S1), a video from the experiment, a graph of velocity time series data (Fig. S2), and a graph of g_2 in a test for randomness (Fig. S3).
[20] P. K. Shukla and A. A. Mamun, *Introduction to Dusty Plasma Physics* (Institute of Physics Publishing, Bristol, 2002).
[21] S. A. Khrapak *et al.*, Phys. Rev. E **72**, 016406 (2005).
[22] Wen-Tau Juan *et al.*, Chin. J. Phys. **37**, 184 (1999).

[23] A. Melzer, M. Klindworth, and A. Piel, Phys. Rev. Lett. **87**, 115002 (2001).
[24] T. E. Sheridan, Phys. Rev. E **72**, 026405 (2005).
[25] B. Liu and J. Goree, Phys. Rev. E **71**, 046410 (2005).
[26] B. Liu *et al.*, Phys. Plasmas **16**, 083703 (2009).
[27] Y. Feng, J. Goree, and B. Liu, Rev. Sci. Instrum. **78**, 053704 (2007).
[28] T. E. Sheridan, M. R. Katschke, and K. D. Wells, Rev. Sci. Instrum. **78**, 023502 (2007).
[29] The small errors in κ and λ_D are due to small errors in the peak frequencies and r_0.
[30] A minor limitation of this method of identifying the modes is that the finite widths of the bandpasses used can allow some leakage of one mode into the bandpass of the other; this accounts for the weak positive correlation in Fig. 4(a) at $v_{x,\alpha} = -v_{x,\beta} = 1.5$ mm/s. We observe leakage of the high frequency mode into the low frequency bandpass, but not vice versa. This observation indicates that a single mode has a spectral peak that is not shaped symmetrically, but instead has a fat tail at low frequencies, as for example the peak in the spectrum of a damped driven harmonic oscillator.
[31] In a test, we also calculated g_2 using velocity data that were filtered the converse way, to exclude contributions in bandpasses centered at the two peaks, and we found that the resulting g_2 was mostly random, unlike Fig. 4. This result is shown in the Supplemental Material [19].
[32] The modes are described not only by frequencies but also by phases, and these phases might vary randomly.